Heliyon 10 (2024) e37927

Contents lists available at ScienceDirect

Heliyon

journal homepage: www.cell.com/heliyon

Research article

Green synthesis of zinc oxide nanoparticles for the industrial biofortification of (*Pleurotus pulmonarius*) mushrooms

Muhammad Bin Ali [a], Tehreema Iftikhar [a,**], Hammad Majeed [b,*]

[a] *Applied Botany Lab, Department of Botany, Government College University, 54000, Lahore, Pakistan*
[b] *Department of Chemistry, University of Management and Technology Lahore (UMT), Sialkot Campus, 51310, Sialkot, Pakistan*

ARTICLE INFO

Keywords:
Zinc oxide nanoparticles
Pleurotus pulmonarius
Mushrooms
Nigella sativa
Fortification
Sustainable Development Goals

ABSTRACT

Zinc malnutrition is major health problem in children and women of reproductive age (WRA) in developing countries. This study aimed to find nutritionally balanced food at an affordable cost. For this purpose, *Pleurotus pulmonarius* (Mushroom) is fortified with zinc oxide nano particles (ZnO-NPs) synthesized from *Nigella sativa* seed extract. ZnO-NPs were characterized using UV visible and FTIR Spectroscopy, SEM-EDX, XRD, PSA and Zeta potentials. ZnO-NPs were sprayed in different concentrations on substrate used for the cultivation of *P. pulmonarius*. Cultivated mushroom fruiting bodies were dried and powdered. Bio absorption of zinc was calculated using atomic absorption spectroscopy. Zinc absorption increased by enhancing the number of nano particles spraying on lingo-cellulosic substrate. The controlled bag had 2.27 ± 0.00 mg of zinc content per 2 g of mushroom powder. The minimum amount (3.46 ± 0.16 mg/2 g of mushroom) of zinc micronutrient was absorbed by the bag having 50 mg spray of ZnO-NPs per Kg of the wheat straw. Maximum amount of bio accumulation was done by bag having 5000 mg spray of ZnO-NPs (10.46 ± 0.08 mg/2 g of mushrooms powder). Zinc fortification had a significant ($p < 0.05$) effect on the uptake of zinc by fruiting bodies. ZnO-NPs at the concentration of 200 mg per kilogram of substrate gave optimized value of biological efficiency [B.E] (40.2 % ± 0.25), while B.E decreased with the increase in ZnO-NPs spray due to bio accumulation of zinc with increased concentration of ZnO-NPs spray.

1. Introduction

The 2023 Sustainable Development Goals (SDGs) report is truly alarming, as most of the SDGs are still lagging, and some have not been addressed by many nations. The survival and well-being of all living species on this planet require urgent and continuous efforts to research and implement the SDGs and to change lifestyle patterns. Climate change, global warming, the use of synthetic diets, chemicals, microfibers, plastics, urbanization, industrial revolutions, and population growth have created numerous health issues for all living species. Humans are responsible for many of these issues due to the non-sustainable approaches of our forefathers. It is now our primary duty to think about future generations and focus our research on achieving the SDGs [1–7].This research work aimed to focus on many SDGs like 2, 3, 12, 13, 17 etc. Zinc is essential for maintenance, growth and development of human tissues, proper

* Corresponding author.
** Corresponding author.
E-mail addresses: dr.tehreema@gcu.edu.pk, pakaim2001@yahoo.com (T. Iftikhar), dyeing@gmail.com, hammad.majeed@skt.umt.edu.pk (H. Majeed).

https://doi.org/10.1016/j.heliyon.2024.e37927
Received 2 August 2024; Received in revised form 12 September 2024; Accepted 13 September 2024
Available online 19 September 2024

functioning of immune system, cognitive activities and reproductive health [8]. Therefore, zinc deficiency can cause problems related to growth, cognitive malfunctioning and enhance the risk of illness and mortality. Due to poor diet in low-income families of developing countries children under five suffer from zinc deficiency [9–12].

ZnO nano particles are GRAS [generally regarded as safe] for human consumption with specific limit of toxicity. Nano Particles show efficient chemical, physical, thermal, mechanical and biological characteristics as analogized to ponderous and bulky materials. Zinc plays a vital role and functions within a particular concentration range in many biological systems of plant. Nano particles have been used frequently in biological fields as it has high solubility, stability, adhesive properties and biocompatibility [13–17].

By using plants for the synthesis of ZnO nano particles give a replacement of non-toxic organic reducing agent, instead of employing toxic chemicals. This method is climate friendly as well as cheap. Nano particles can be used for bio-fortification replacing fertilizers as they have particle size of 100 nm or less. This gives them a higher surface area, more absorption availability intake to mushroom mycelium. Several physical, chemical and biological methodologies have been known for the preparation of nano particles, but biological methods are more suitable as it involves organic plants. Other processes involve high thermal conditions, acidic pH and hazardous chemicals which are very toxic and unsafe. Plant synthesis of nano particles is significant to its antimicrobial and eco-friendly nature. Plant based nano particles formation is preferable for large scale production, in which plant extract is used as a reducing agent [18–22].

Edible mushrooms contain high protein fibers and vitamin content which has a lot of health benefits. Moreover, they have health fostering compounds with antimicrobial, antioxidant, anti-inflammatory and anti-tumor characteristics. Recent studies have revealed that mushrooms have a distinctive and exceptional capability to bio accumulate metals from their external environment. Harvested mushrooms are useful for biofortification of micronutrients to remove their deficiency in our daily life [23,24].

ZnO-NPs have more tendency to absorb than chemical sources as they have smaller particle size and larger surface area to absorb. The present piece of work is linked with SDG 2, 3, 12 and 13. It is an effort to produce zinc-fortified *Pleurotus pulmonarius* mushroom having optimized amount of zinc micro-nutrients to reduce zinc malnutrition in children and WRA in developing countries. By optimizing zinc micronutrient amount in *Pleurotus pulmonarius*, its lesser quantity can be used to promote health related to physical, mental growth and better functioning of immune system. Wheat straw has been the major agricultural waste in the regions where wheat is the major agricultural crop. This work is useful to see the basis for using agri-waste as ligno-cellulosic source for the cultivation of *Pleurotus pulmonarius*. The present work is designed to fortify *Pleurotus pulmonarius* with ZnO nanoparticles [ZnO-NPs] synthesized from *Nigella sativa* seed extract.

Studies have demonstrated that by improving nutrient uptake, stress tolerance, and general metabolic activity, the application of nanoparticles, such as zinc oxide nanoparticles (ZnONPs), in agricultural operations can stimulate the growth of plants and fungi. Zinc oxide nanoparticles (ZnONPs) derived from *Nigella sativa* have the potential to enhance development metrics in *Pleurotus pulmonarius*, including mycelial growth rate, spawn run time, and fruiting body formation. This could result in increased yields and better-quality mushrooms. Because *Nigella sativa* serves as both a source of bioactive compounds that can combine to improve the nutritional value and antimicrobial qualities of the fortified mushrooms and a reducing agent for green synthesis, it makes reason to use it to prepare zinc nanoparticles for the purpose of fortifying mushrooms. Using fortified food products, this method not only supports sustainable agriculture practices but also offers a highly bioavailable form of zinc to improve human health. Utilizing such cutting-edge techniques demonstrates how food science and nanotechnology are integrating to address micronutrient deficiencies and enhance crop quality in a safe and natural way [25–27].

This is a novel approach: *Nigella sativa* extract and zinc acetate were used to synthesize zinc nanoparticles, which were then used to biofortify mushrooms (*Pleurotus pulmonarius*). This study combines green synthesis with ecologically friendly nanoparticle synthesis by employing *Nigella sativa*. Some studies explored the use of agriculture waste material for the synthesis of zinc nanoparticles [28–31]. By providing the advantages of ZnONPs for more effective zinc delivery in mushrooms, it enhanced nutritional delivery. These nanoparticles' dual-function fortification gives mushrooms improved antibacterial qualities in addition to zinc biofortification. Because the ideas of sustainable agriculture, nanotechnology, and green chemistry are being used in this research, it represents a cross-disciplinary integration. This research has the potential to make a substantial contribution to human nutrition, sustainable agriculture practices, and scientific knowledge. It may also pave the way for the development of novel functional food products.

It possesses several distinctive as well as unusual qualities. A few factors, such as the synthesis technique, the combination of materials employed, and the biofortification application, can be utilized to evaluate the uniqueness of this work. Although studies on the environmentally friendly manufacturing of nanoparticles using different plant extracts have been conducted, *Nigella sativa*, which is abundant in bioactive substances such phenolics, flavonoids, and thymoquinone, provides a special blend of antibacterial activity and reducing power. The interesting aspect of this is that *Nigella sativa*'s phytochemicals are combined to regulate the synthesis parameters of ZnONPs, possibly producing distinct particle morphology, size, and surface characteristics that are ideal for biofortification. While adding vital micronutrients like zinc to crops and mushrooms through biofortification is a well-known method of addressing nutritional deficiencies, using ZnONPs produced environmentally is a novel way to achieve this goal. When it comes to zinc, ZnNPs are more bioavailable than traditional zinc salts (like zinc sulfate or zinc acetate). There hasn't been any research done on ZnNP application in mushroom fortification by using *Nigella sativa*. Due to their large surface area and superior cellular absorption, green-synthesized ZnNPs proved to be a more effective bio fortifier for increasing the zinc content of mushrooms. This strategy may produce new insights into how ZnNPs interact with the mycelium and fruiting bodies of mushrooms. It is commonly known that *Nigella sativa* possesses antibacterial, antioxidant, and immunomodulatory qualities. By incorporating these characteristics into the ZnNP production process, it is possible to produce nanoparticles with increased biological activity. Beyond just providing zinc supplementation, these physiologically active ZnNPs fortifying mushrooms may have other health benefits. For instance, they might lengthen the mushrooms' shelf life by lowering microbial contamination, and they might also increase their therapeutic value by having a combined

antioxidant and antibacterial action. This study offers a fresh, more effective way to incorporate important elements like zinc into everyday meals. Zinc shortages are common in many countries, and a novel dietary supplement to address them is mushrooms supplemented with ZnNPs made from *Nigella sativa*. Using *Nigella sativa* for the green synthesis of ZnNPs is a more environmentally friendly and sustainable way than typical chemical methods, which frequently use toxic stabilizers and reducing agents. The study could also lead to new insights into the uptake mechanism of ZnNPs in fungal cells, their effects on mushroom physiology, and their potential to enhance the nutritional and medicinal properties of mushrooms.

2. Materials and methods

2.1. Materials

Wheat straw, seeds of *Nigella sativa* was supplied by Innovation Research Centre of Coural Associates and get verified (voucher specimen # LCW/BOT/1021). Inno Tech Technologies UV–visible spectrophotometer (Inno-DG6500), FTIR spectrophotometer (Carry 630 Agilent), XRD (Bruker D8 advance Germany), SEM with EDX (SEM/EDX model: EVO LS10 Zeiss, Germany), Zinc acetate dihydrate (Merck), HCl (37 % purity by Merck), atomic absorption spectroscopy (Model: AA 7000 F with Autosampler and Hydride Vapour Generator, Shimadzu, Japan). All the chemicals (both analytical and commercial grade) were supplied by Coural Associates.

2.2. Methods

2.2.1. Preparation of Nigella sativa seed extract and its zinc nanoparticles

Seeds of *Nigella sativa* was first rinsed in distilled water four times. The seeds were dried and ground into a fine powder. Twenty grams of the powder were taken in 200 mL of distilled water and boiled for 30 min. After cooling, the solution was filtered, and the filtrate was stored for further use. Then 500 mL of 0.25 M zinc acetate solution was prepared. 160 mL of seed extract was added to the zinc acetate solution dropwise under continuous stirring at 60 °C for 2 h. During stirring, the pH was maintained at 12 using a 10 % sodium hydroxide solution. The plant extract acted as a reducing agent, reducing zinc acetate to ZnO nanoparticles and formed yellow precipitates. The mixture was centrifuged at 179×*g* for 15 min, and then the pellet was separated on a petri plate and dried at 60 °C for 2 h. The dried pellet was scraped and calcined at 400 °C for 4 h [32–35].

Using the natural reducing and stabilizing agents found in plant extracts, the synthesis of zinc oxide (ZnO) nanoparticles from zinc acetate is demonstrated in this interesting case study of green nanoparticle synthesis. The phytochemicals in the extract aid in the bioreduction process used to create ZnO nanoparticles from *Nigella sativa*. ZnO nanoparticles are synthesized using zinc acetate dihydrate ($Zn(CH_3COO)_2{\cdot}2H_2O$) as a precursor. It separates into zinc ions (Zn^{2+}) and acetate ions (CH_3COO^-) when dissolved in water. Zinc ions, or Zn^{2+}, are the building blocks that finally result in ZnO nanoparticles. The seeds of *Nigella sativa*, known as black cumin, are rich in bioactive substances (thymoquinone, flavonoids, phenolic acids, tannins, saponins, alkaloids) with reducing, capping, and stabilizing qualities. Zinc ions (Zn^{2+}) can be reduced by these phytochemicals to produce zinc oxide (ZnO). Zn^{2+} ions are reduced to Zn atoms by the phytochemicals (mostly flavonoids and phenolics) when the *Nigella sativa* aqueous extract is added to the zinc acetate solution. These reduced zinc atoms can combine with oxygen-containing molecules in the solution to generate ZnO. An intermediate known as zinc hydroxide ($Zn(OH)_2$) may be produced during the reduction process.

$$Zn^{2+} + 2OH^- \rightarrow Zn(OH)_2$$

Upon heating/stirring, $Zn(OH)_2$ undergoes dehydration to form ZnO:

$$Zn(OH)_2 \rightarrow ZnO + H_2O$$

This conversion is supported by the extract's organic components rapid oxidation. Flavonoids and polyphenols, which are stabilizing (capping) agents as well as reducing agents, are found in *Nigella sativa*. These substances adhere to the surface of the freshly generated ZnO nanoparticles, inhibiting their growth and causing them to not aggregate, which results in a more homogeneous size distribution. Green chemistry is supported by the use of *Nigella sativa* extract as a reducing and stabilizing agent. It offers a sustainable and eco-friendly way to synthesize nanoparticles and there is no need to use dangerous chemicals. This method of producing ZnO nanoparticles by utilizing *Nigella sativa* is a promising area of study, offering a more environmentally friendly way to produce nanoparticles with potential uses in a variety of sectors, such as chemistry, biochemistry, biotechnology, agriculture, food, and medicine.

2.2.2. Characterization and analysis

ZnO-NPs were characterized by the following techniques.

2.2.2.1. UV visible spectroscopy. The green synthesized zinc oxide nanoparticles of plant seed extract were examined by using the UV Visible spectroscopy. The maximum absorption wavelength (λ max) was check by using double beam spectrophotometer.

2.2.2.2. FTIR analysis. FTIR analysis of synthesized plant-based zinc NP is mandatory to evaluate the phytochemical presence, and it is mandatory to check the confirmation of zinc nanoparticle formation.

2.2.2.3. PXRD analysis. The powder XRD analysis is mandatory for the evaluation of zinc nanoparticle formations. It also shows the crystallinity and amorphous nature of synthesized zinc nanoparticles with plant-based material. The obtained peaks were the characteristics of zinc nanoparticles, 2θ values (along the X axis) gives the estimation of each peak position and were compared with the standard JCPDS data. We calculated the FWHM (full width half maxima) by measuring the width of each peak at half of its maximum intensity. After calculating FWHM and 2θ, we used Debye Scherrer equation to evaluate the crystalline size of nanoparticles evaluation confirmation and compared with the data of SEM. The Scherrer equation estimates the crystallite size from the broadening of XRD peaks. It relates the size of the crystallites to the width of the diffraction peaks.

The equation is:

$$D = K\,\lambda / \beta \cos\theta,$$

where as D is the crystalline size, K is the shape factor (mostly around 0.9), λ is the X ray wavelength (for Cu Kα radiation, λ = 0.154 nm), β is the full width at half maximum (FWHM) of the peak in radians, θ is the Bragg angle (between the incident X ray and the reflecting crystal planes, which is half of the 2θ value where the peak occurs [36].

We started with the X ray diffraction pattern identification, peaks and their positions. Then we calculated the d spacing using Bragg's law ($d = n\,\lambda/2 \sin\theta$, whereas n is 1 for the first order reflection). Then we estimated the crystalline size (D) with the help of Scherrer equation which include the calculation of β (FWHM) of each peak, then conversion of β degree into radian by using the formula $\beta\ (\text{radians}) = \beta\ (\text{degrees}) \times (\pi/180)$

2.2.2.4. SEM-EDX analysis. Scanning Electron Microscopy was performed with Energy dispersive X rays' spectroscopy. SEM provided detailed images of the surface morphology of the nanoparticles. Zinc oxide nanoparticles synthesized using *Nigella sativa* seed extract, the SEM images also revealed the size, shape, and distribution of the ZnO nanoparticles. The surface texture of the nanoparticles was also observed, to check any agglomeration or uniformity in the particle distribution. SEM also showed the degree of aggregation of the ZnO nanoparticles, which was important for understanding their stability and dispersion.

EDX, coupled with SEM, provided elemental composition analysis of the sample. Peaks corresponding to elements from the *Nigella sativa* seed extract including zinc nanoparticles, indicated the residual organic material from the seed extract. Elemental mapping provided a visual distribution of all the elements across the synthesized sample to show uniformity. The relative intensity of element peaks indicated the purity. Additional/unexpected peaks indicated the presence of impurities or residues from the synthesis process.

Fig. 1. Biofortification process of *Pleurotus pulmonarius*.

2.2.2.5. Particle size analyser. A particle size analyzer is required for determining the size distribution of the synthesized zinc oxide nanoparticles. It provides a detailed size distribution profile of the nanoparticles, indicating the presence of any agglomerates or a broad size range. It calculates the average particle size, which is important for understanding the properties and potential applications of the nanoparticles. Consistent particle size distribution is essential for ensuring the reproducibility and reliability of the synthesis process. Different applications may require different particle sizes. For example, smaller nanoparticles may have higher surface area and reactivity, which can be beneficial for certain applications.

To perform a particle size analysis, we used Dynamic Light Scattering (DLS), which measures the size of nanoparticles in a solution by analyzing the scattering of light. First the zinc nanoparticles dispersed in distilled water. Then sonicated the suspension for 25 min to break up any particle aggregates. Then the suspension was filtered. The particle size analyzer was started and allowed it to stabilize. Then the temperature was set at 25 °C and selected the laser wavelength at 800 nm. Then injected the prepared nanoparticle suspension into the sample cell of the particle size analyzer. The instrument emitted a laser beam into the sample, and the light scattered by the particles will be measured at different angles. DLS measured the fluctuations in the scattered light caused by the Brownian motion of particles in the suspension. These fluctuations are analyzed to determine the hydrodynamic diameter of the nanoparticles [37,38].

2.2.2.6. Zeta potential analysis. Zeta potential analysis measures the surface charge of nanoparticles in a suspension. It provides information about the stability and dispersibility of nanoparticles. Zeta potential indicates the degree of electrostatic repulsion between particles. High zeta potential values (positive or negative) suggest that the particles are likely to repel each other, leading to a stable suspension with less aggregation. It provides information on the surface charge properties of nanoparticles, which can influence interactions with biological systems, making it beneficial for biomedical applications. Understanding the zeta potential helps in optimizing the synthesis process to achieve stable colloidal dispersions, which are essential for applications like drug delivery, where uniform particle dispersion is critical. The surface charge can affect how nanoparticles interact with their environment, including other particles, solvents, and biological systems. This is vital for applications in environmental remediation, agriculture, and medicine [39–41]. Fig. 1 demonstrated complete research work.

2.2.3. Zinc fortified mushroom preparation

Wheat straw was rinsed in distilled water and soaked overnight. The substrate was then dried by spreading it on a table under constant airflow. After reaching the optimized moisture retention level, 100 g of substrate was filled into each polypropylene bag [42]. Each bag was sprayed with ZnO-NPs at different concentrations (0 mg, 50 mg, 100 mg, 200 mg, 400 mg, 800 mg, 1000 mg, 2000 mg, 3000 mg, 4000 mg, and 5000 mg) using a spray bottle. The bags were then sterilized at 121 °C and 15 psi for 15 min. After cooling, the bags were inoculated with mother spawn of *Pleurotus pulmonarius*. The bags were incubated in the dark for 25 days at 25 °C [43]. After completion of vegetative stage (complete covering of white mycelium) growing bags were cut at different sites. The environmental conditions were kept as follows constant light, air flow, humidity increased up to 90 % and temperature was dropped to 16–18 °C [44]. After 3–4 days fruiting bodies started sprouting. Harvesting was carried out after proper gill opening. Fresh mushrooms were harvested and dried at 35 °C for 2 days. Dried mushrooms were grounded to powdered form.

Pleurotus pulmonarius (2 g) was taken in a crucible and placed on a hot plate at 250 °C until completely charred. The crucible was then placed in a muffle furnace at 550 °C for 2 h. After ashing, the sample was digested by adding 25 mL of 5M HCl. This process was performed in a fume hood. After digestion, the mixture was filtered using Whatman filter paper no. 1 into a volumetric flask and filled to the top with distilled water. Zinc oxide quantification was done using atomic absorption spectroscopy. A standard curve was obtained by preparing a standard solution of zinc at different concentrations (0 ppm, 0.5 ppm, 1 ppm, 1.5 ppm, 2 ppm, 2.5 ppm, 3 ppm, 3.5 ppm, and 4 ppm). The amount of zinc was determined by comparing the absorption values of the sample with the standard curve values [45].

2.2.4. Mushroom characterization

2.2.4.1. Biological efficiency (B.E). Bio-conversion efficiency was calculated by using following formula:

$$\text{Biological efficiency} = [\text{F.W (g)}/\ \text{D.W (g)}] \times 100$$

F.W is fresh weight of harvested mushrooms in grams; D.W is dried weight of lingo-cellulosic substrate in grams [44].

2.2.4.2. Color analysis. Colorimeter was used for the skin color analysis of fortified fruiting bodies of *Pleurotus pulmonarius* which was done in Food Science and Technology Lab, University of Lahore, Lahore, Pakistan. Colorimeter provided 5 values: L*, a*, b*, c* and h*. L* measured the lightness from black to white on the scale of 0–100, a* ranging from +60 redness to – 60 greenness and b* ranging from +60 yellowness to - 60 blue represented the chromaticity, c* showed the saturation or intensity of color. c* showed the distance of a color from the neutral axis in the lab color space and h* showed the hue of color in degrees [34,35,46,47].

2.2.5. Statistical analysis

Data was analyzed using SPSS software version 21. The data was expressed as the mean ± standard deviation of measurements from triplicate experiments. ANOVA was used to determine levels of significance ($p < 0.05$).

3. Results

3.1. Plant based zinc nanoparticles evaluation

Formation of nano particles was confirmed by change in colour of solution from brown to light yellow when seed extract was added, which reduces the zinc acetate into zinc oxide nanoparticles.

3.1.1. UV visible spectroscopy of zinc nanoparticles (ZnO-NPs)

Nigella sativa seed extract acted as a reducing agent when poured into zinc acetate solution, which reduced the zinc salt to nano particles, indicating yellow precipitates. This solution was analyzed under ultraviolet spectroscopy confirming the synthesis of ZnO-NPs and revealed the stability and optical activity of nanoparticles. The UV Visible spectroscopy range started from near UV (200 nm) to 800 nm. Maximum absorption spectrum was obtained at 360 nm confirming the formation of ZnO nano particles as shown in (Fig. 2).

The size of the ZnO nanoparticles synthesized using the *Nigella sativa* seed extract is in the nanometer range. At this nanoscale, the electrons in the ZnONPs are confined, leading to a phenomenon called the quantum confinement effect. This effect causes a blue shift in the absorption spectrum, resulting in the observed highest peak at 360 nm. The maximum absorbance at 360 nm is due to the electron transport phenomenon from the valence band of ZnO nanoparticles to the conduction bands i.e. Zn (3d orbital) →O (2p orbital). Smaller nanoparticles tend to have a blue-shifted absorption peak compared to larger nanoparticles. The peak at 360 nm suggests that most synthesized ZnO nanoparticles have a size distribution in the range where the quantum confinement effect is prominent. Also, the band gap energy of ZnO is approximately 3.37 eV (in bulk mass scale), which corresponds to an absorption wavelength of around 368 nm. The observed peak at 360 nm is close to this theoretical value, indicating that the synthesized ZnO nanoparticles have a band gap energy consistent with the bulk ZnO material. The surface defects and impurities in the ZnO nanoparticles can also contribute to the observed absorption peak. These defects and impurities can introduce additional energy levels within the band gap, leading to the absorption peak at a slightly lower wavelength than the theoretical value (2.91 eV). The energy bandgap of the ZnO nanoparticles was calculated using the Tauc equation [(αhυ) ¼ A(hυ-Eg)], where hυ is the photon energy, Eg is the energy bandgap, A is the band tailing parameter, and α is the absorption coefficient [2–4,33,48].

3.1.2. FTIR spectroscopy

The FTIR spectrum of *Nigella sativa* seed extract based zinc oxide nanoparticles shows several characteristic peaks. Specifically, the O-H stretching vibrational mode of water and alcohol molecules was observed with peaks at 3861 cm^{-1} and 3746 cm^{-1} in the plant seed extract. The C=O stretching vibration of the carboxyl group (-COOH) was characterized by a peak at 2367 cm^{-1}, indicating the presence of carboxylic acids and ester compounds in the extract. The C=C stretching vibrational mode of the aromatic ring (peak at 1653 cm^{-1}) and C-O stretching mode (at 1395 cm^{-1}) are most probably due to the presence of phenolic or flavonoid compounds in the plant material. The C-O stretching mode of the aliphatic chain was confirmed with a peak at 1037 cm^{-1}, which may be due to the presence of aliphatic alcohols and ethers. The Zn-O stretching mode of the ZnO nanoparticles was observed with peaks at 597 cm^{-1} and 490 cm^{-1} (Fig. 3).

3.1.3. X-ray diffraction analysis

XRD peaks confirming the purity and showing hexagonal (wurtzite) crystalline structure of ZnO-NPs (Fig. 4). The XRD pattern shows several distinct peaks, which are characteristic of crystalline zinc oxide (ZnO) nanoparticles. The major peaks can be identified at approximately 2θ values of 31.7°, 34.4°, 36.2°, 47.5°, 56.6°, 62.9°, 68.0°, 69.1°. These peaks match the standard Joint Committee on Powder Diffraction Standards (JCPDS) card No. 01-080-0074 for the hexagonal wurtzite structure of ZnO. The peaks at 2θ values correspond to the (100), (002), (101), (102), (110), (103), (200), and (112) crystal planes of ZnO, respectively. These planes are indicative of the hexagonal phase of ZnO, which is the most thermodynamically stable form. The sharp and intense peaks indicate good crystallinity of the ZnO nanoparticles, suggesting a well-ordered crystalline structure with minimal defects.

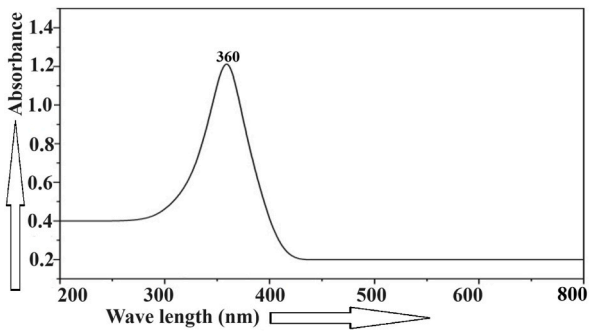

Fig. 2. UV Visible spectroscopy analysis of synthesized plant-based ZnO-NPs.

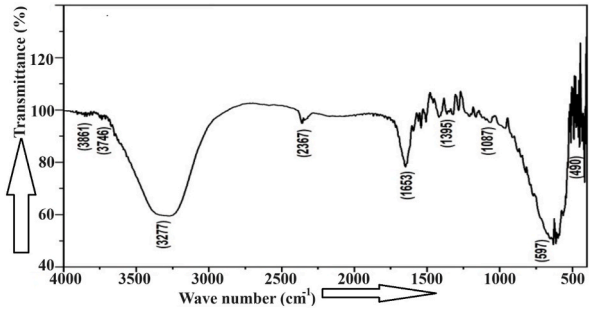

Fig. 3. FTIR spectrum of *Nigella sativa* plant ZnO-NPs.

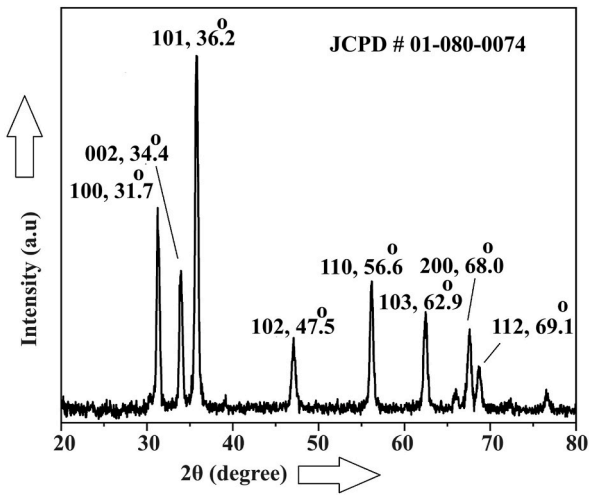

Fig. 4. XRD graph of plant zinc NPs.

3.1.4. Particle size analyzer

After calcination, the sample was analyzed for Particle Size Analyzer which revealed that the diameter of zinc oxide nano particles was 80 nm (Fig. 5). This graph in Fig. 5 represents the particle size distribution of zinc nanoparticles synthesized using zinc acetate and *Nigella sativa*. The x-axis shows the particle diameter in nanometers (nm), while the y-axis shows the relative frequency (%), indicating the proportion of particles with a particular size. The Main Peak is around 100 nm. The sharp peak indicates that most nanoparticles have a diameter close to 100 nm. This suggests a uniform particle size distribution for most of the sample. A narrow distribution indicates good control over particle size during synthesis. Secondary Peak which is around 150–175 nm. There is a minor peak or "shoulder" around 150–175 nm, showing the presence of some larger particles, but at a much lower frequency (around 1–2% relative frequency). This might result from agglomeration or incomplete reduction during the synthesis process.

The software calculated the particle size distribution based on the intensity of the scattered light.

The main peak (as seen around 100 nm) corresponds to the average particle size, while secondary peaks indicate the presence of larger or aggregated particles. The result is typically presented as a size distribution graph, showing the relative frequency of particles at different diameters, as in the provided graph. This method is widely used due to its sensitivity and ability to measure particles in the

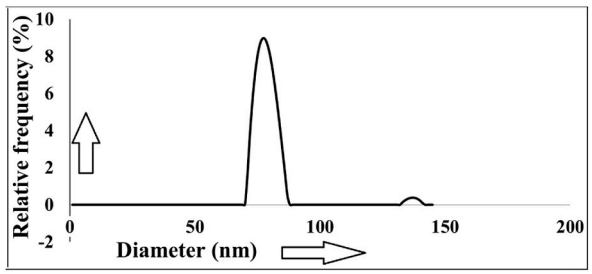

Fig. 5. Particle size analysis plant based ZnO-NPs.

nanoscale range.

3.1.5. Scanning electron microscopy

Scanning electron microscope showed the spherical shape of zinc oxide nano particles with the size from 69 to 100 nm (Fig. 6a and b). In SEM the average size of green synthesized ZnO-NPs was 69–100 nm, confirming the diameter 100 nm or lesser. The shape of nano particles was spherical. Both temperature and amount of extract should be higher to obtained lesser size of NPs.

Fig. 6a-b. SEM characterization of ZnO-NPs 6a) shape and diameter 6b) Histogram showing average diameter of ZnO-NPs. XRD analysis showed that ZnO nano particles synthesized from *N. sativa* seed extract were free from impurities and confirmed by comparing with standard ZnO JCPDS.

EDX spectrum showed the purity of ZnO-NPs. (Fig. 7 and Table 1).

3.1.6. Zeta potential

Zeta potential of zinc oxide nano particles was obtained at −8.52 mV shown in Fig. 8. The negative value of apparent zeta potential confirmed the good colloidal stability of ZnO-NPs. Zeta potential of ZnO-NPs prepared from *Nigella sativa* revealed good stability at −8.52 mV. Surface charge is negative due to the presence of strong binding tendency between extract components and ZnO-NPs, this helps to lower the chances of aggregation and enhance the stability of ZnO-NPs.

3.2. Mushroom characterization

3.2.1. Atomic absorption spectroscopy

The zinc content of biofortified mushrooms was analyzed using atomic absorption spectroscopy as shown in Table 2 and Fig. 9. The uptake of zinc increased as the spraying of ZnO-NPs increased. In controlled substrate formulation 2.27 ± 0.00 mg of Zn was present per 2 g of mushroom powder. The maximum amount of Zinc (10.46 ± 0.08) was present in 5 g of substrate formulation and minimum amount of Zinc (3.46 ± 0.16) was obtained in 50 mg formulation. B.E (%) was increased with gradual increase in NPs concentration and decreased after 200 mg zinc oxide formulation due to the abundance of Zn micronutrient which has negatively affected the growth of mushroom. Maximum B.E (40.2 ± 0.25) was obtained at 200 mg formulation and minimum B.E (22.0 ± 0.57) was calculated at 5000 mg formulation.

Total Zn (mg)/2 g of mushroom and biological efficiency (%) are mean ± S.D of triplicates values (n = 3); Fortification of zinc to growing substrates had a significant ($p < 0.05$) effect on the uptake of zinc micronutrient. (Determined by using One-way ANOVA, Post-hoc-Tukey test, 95 % confidence limit). AAS Table 2 showed the zinc content present in the fortified mushrooms, which was quantified using Atomic Absorption Spectroscopy. 100 mg zinc NPs spray gave maximum B.E on given substrate. With the increase in ZnO nanoparticles spray yield of *Pleurotus pulmonarius* decreased. The least of the yield obtained at 5g of spray, as excess fortification of NPs will negatively impact the B.E. Bio absorption of zinc oxide increased by enhancing the amount of ZnO-NPs spray.

A plot of mean values revealed that as the concentration of ZnO increased in the lingo-cellulosic substrate the amount of Zn uptake by fruiting bodies also increased.

X-axis determining the groups (zinc fortified substrate bags with ZnO nano particle amount ranging from 0 mg to 5000 mg) while Y-

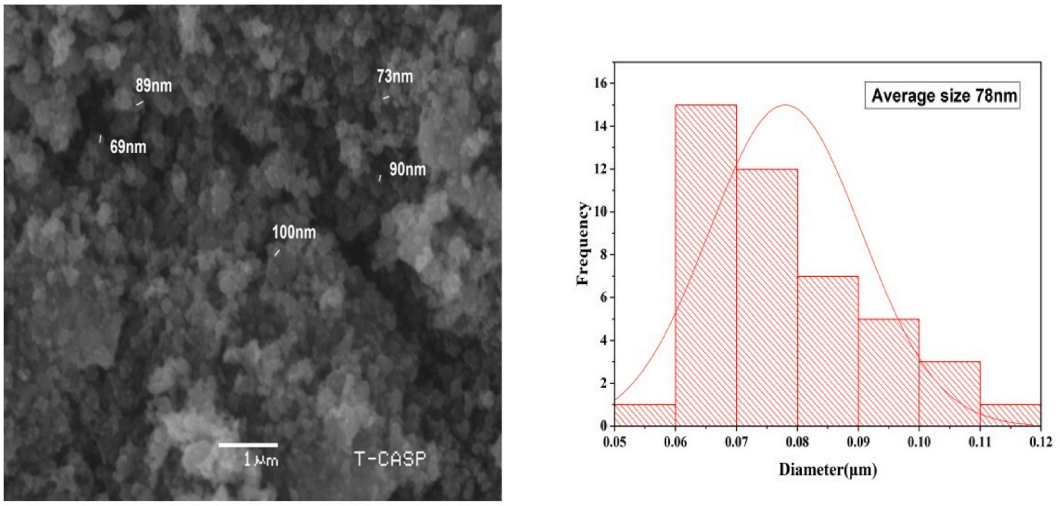

a **b**

Fig. 6. a showing spherical shape and diameter of ZnO NPs
b. Histogram showing the average diameter.

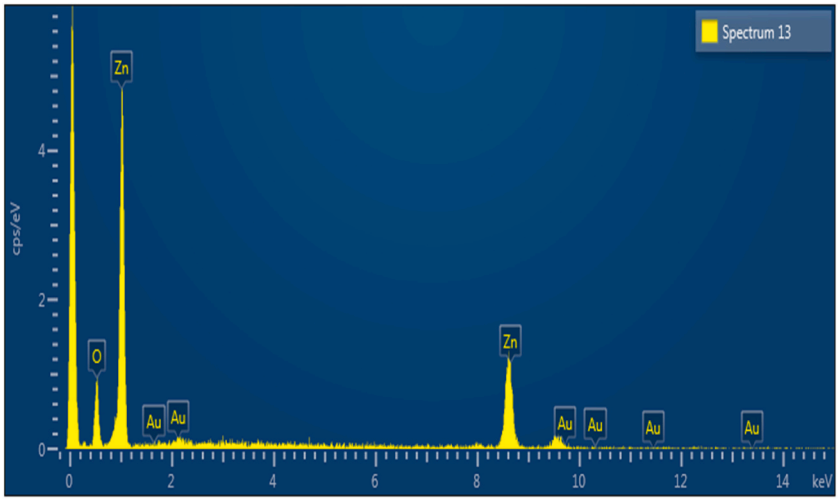

Fig. 7. EDX analysis of ZnO-NPs showing two higher peaks of Zn showing the relative abundance and purity of Zn.

Table 1
Table showing relative amount (%) of zinc (77.53), oxygen (20.72) and Au (1.75).

Element	Line Type	Apparent Concentration	k Ratio	Wt%	Wt% Sigma	Standard Label	Factory Standard
O	K series	18.78	0.06319	20.72	1.19	SiO_2	Yes
Zn	K series	58.51	0.58509	77.53	1.44	Zn	Yes
Au	M series	0.82	0.00823	1.75	1.06	Au	Yes
Total:				100			

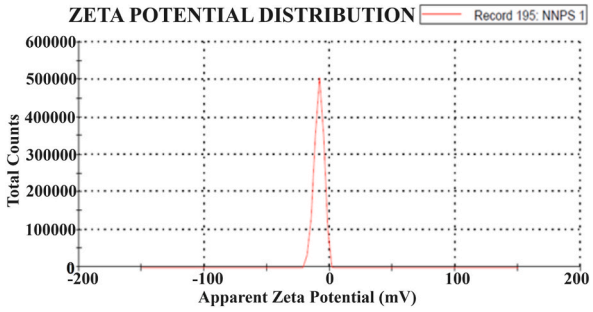

Fig. 8. Zeta potential of zinc oxide nano particles.

Table 2
Representing total uptake of zinc (mg) by fruiting bodies and B.E (%).

Substrate formulation/kg	Total Zn (mg)/2 g of mushroom	Biological efficiency (%)
0 mg ZnO	2.27 ± 0.00	29.0 ± 0.20
50 mg ZnO	3.46 ± 0.16	30.0 ± 0.26
100 mg ZnO	4.29 ± 0.13	32.0 ± 0.17
200 mg ZnO	4.76 ± 0.19	40.2 ± 0.25
400 mg ZnO	5.26 ± 0.16	26.0 ± 0.26
800 mg ZnO	5.73 ± 0.14	25.4 ± 0.20
1000 mg ZnO	6.20 ± 0.13	24.8 ± 0.11
2000 mg ZnO	7.64 ± 0.26	24.0 ± 0.10
3000 mg ZnO	8.17 ± 0.15	23.6 ± 0.21
4000 mg ZnO	9.28 ± 0.14	23.2 ± 0.28
5000 mg ZnO	10.46 ± 0.08	22.0 ± 0.57

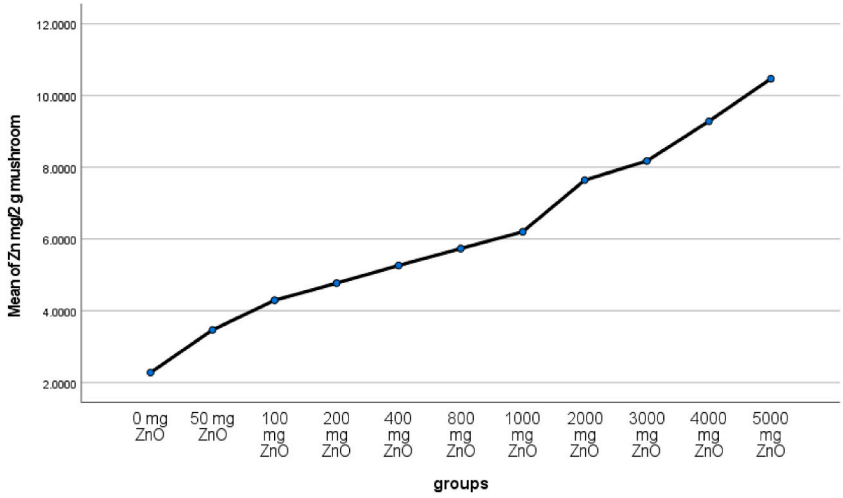

Fig. 9. Atomic absorption spectroscopy results.

axis showing the amount of zinc absorbed by the growing mushroom on the specific bags.

3.2.2. Color analysis

The color analysis showed the difference in colors of bio-fortified mushrooms. L*: Degree of whiteness decreased from control to increased concentration in the fruiting bodies of Zn uptake. a* showing degree of redness to blueness, which is higher having higher amount of nano particle exposure. b* representing the degree of yellowness which is highest in control because *Pleurotus pulmonarius* has a little yellow texture which has decreased with more exposure and uptake of ZnO NPs. c*: showing the saturation of colors which is lowest in control and increase with the increase in Zn uptake due to change in color intensity. h* showing hue of color in angle, which is higher in control and decreased as the shade diminishes with absorption of Zn (shown in Fig. 10 and Table 3).

In Table 3, the effect of ZnO-NPs on the color of fruiting bodies. Cultivation substrate fortified with various concentrations of ZnO NPs, From Control to mushroom sample with ZnO NPs fortification, 50 mg, 100 mg, 200 mg, 400 mg, 800 mg, 1000 mg, 2000 mg, 3000 mg, 4000 mg and 5000 mg. There was a significant difference ($p < 0.05$) of mean in triplicate ($n = 3$) values with ±S.D shown in form of L*, a*, b*, c* and h* by samples grown on different concentrations of biofortified substrate.

Excessive use of zinc micronutrient can be dangerous because it exceeds the required daily intake and may result in toxicity. This could cause problems related to growth, so it is advised that children having age 6–23 months should take 4–5 mg of zinc per kg of diet. On the other hand, adults should consume about 6 mg of zinc per kg of daily diet.

4. Conclusion

This research focused on addressing the critical issue of zinc malnutrition, particularly in children and women of reproductive age in developing countries. The study successfully synthesized zinc oxide nanoparticles (ZnO-NPs) from *Nigella sativa* seed extract for the industrial biofortification of mushrooms, specifically *Pleurotus pulmonarius*, to create a nutritionally balanced and affordable food source. Various characterization techniques such as UV visible and FTIR Spectroscopy, SEM, EDX, XRD, PSA, and Zeta potentials were employed to analyse the synthesized ZnO-NPs, ensuring their quality and properties for biofortification purposes. The bio absorption of zinc into the mushroom fruiting bodies was quantified using atomic absorption spectroscopy, with results showing a significant increase in zinc absorption with higher concentrations of ZnO-NPs sprayed on the substrate used for cultivation. The study revealed that controlled spraying of ZnO-NPs on the lingo-cellulosic substrate led to an optimal zinc content in the mushroom powder, with the highest bioaccumulation achieved at 5000 mg spray of ZnO-NPs per kilogram, significantly affecting the uptake of zinc by the fruiting bodies. The research demonstrated that the concentration of 200 mg of ZnO-NPs per kilogram of substrate provided the highest biological efficiency (B.E) of 40.2 % ± 0.25, indicating an optimized value for biofortification purposes, while a decrease in B.E was observed with higher concentrations of ZnO-NPs due to increased zinc bioaccumulation. Overall, the research work highlighted the potential of green synthesis of *Nigella sativa* zinc nanoparticles for the industrial biofortification of mushrooms, offering a sustainable solution to combat zinc deficiency and enhance the nutritional value of food sources in regions facing malnutrition challenges. In the modern world, it is impossible to conduct any type of business without a sustainable approach. The Industrial Revolutions 5.0 and 6.0 intensively demand a focus on the circular economy, zero waste, and net-zero emissions. We must address global warming to avoid endangering humanity. The implementation of intelligent manufacturing techniques in all types of research and industrial practices is also unavoidable due to the high market demand for cost-effective, right-first-time production with minimal batch-to-batch variation and sustainable industrial practices.

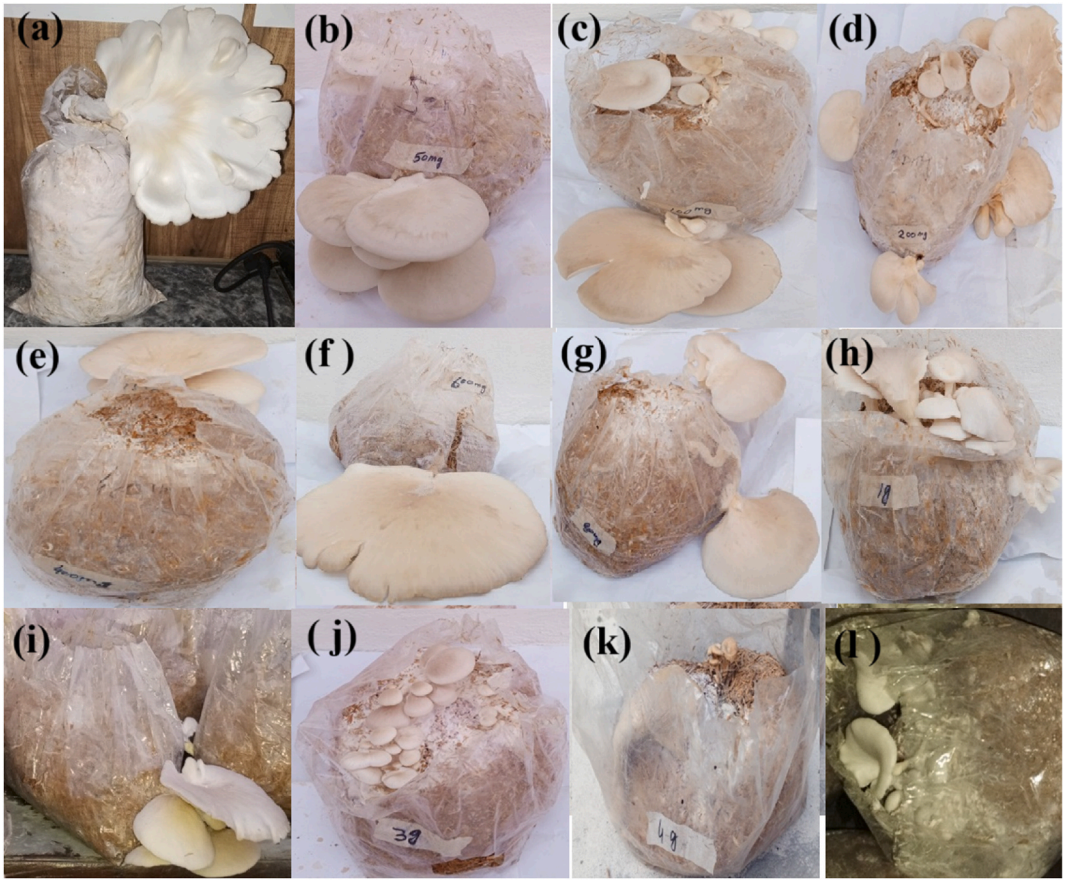

Fig. 10. (a–l). Effect of zinc oxide nano particles on the color of mushroom *Pleurotus pulmonarius* fruiting bodies: a- Control, b- 50 mg, c- 100 mg, d- 200 mg, e– 400 mg, f- 600 mg, g- 800 mg, h- 1000 mg, i- 2000 mg, j- 3000 mg, k- 4000 mg, l- 5000 mg.

Table 3
Color analysis of bio-fortified mushroom samples.

Samples	L*	a*	b*	c*	h*
Control	77.56 ± 0.33	6.70 ± 0.08	36.81 ± 0.10	27.51 ± 0.09	79.64 ± 0.06
50 mg	41.43 ± 0.22	7.62 ± 0.12	33.82 ± 0.09	29.200 ± 0.10	76.75 ± 0.08
100 mg	35.67 ± 0.27	11.55 ± 0.11	30.50 ± 0.26	29.33 ± 0.10	75.86 ± 0.11
200 mg	30.40 ± 0.19	11.84 ± 0.08	29.66 ± 0.15	30.73 ± 0.10	74.54 ± 0.18
400 mg	25.34 ± 0.10	12.22 ± 0.09	28.15 ± 0.12	32.55 ± 0.09	73.48 ± 0.16
600 mg	17.18 ± 0.18	14.85 ± 0.06	27.83 ± 0.08	33.23 ± 0.09	72.83 ± 0.07
800 mg	15.19 ± 0.12	15.58 ± 0.17	25.40 ± 0.08	35.41 ± 0.08	69.15 ± 0.11
1000 mg	12.65 ± 0.18	17.14 ± 0.10	24.24 ± 0.14	37.65 ± 0.12	68.16 ± 0.13
2000 mg	11.22 ± 0.12	19.77 ± 0.11	23.25 ± 0.08	38.75 ± 0.13	65.25 ± 0.12
3000 mg	9.64 ± 0.23	21.16 ± 0.15	24.46 ± 0.12	39.87 ± 0.08	64.64 ± 0.23
4000 mg	3.25 ± 0.13	23.86 ± 0.08	21.76 ± 0.11	41.22 ± 0.10	64.32 ± 0.13
5000 mg	2.41 ± 0.13	24.72 ± 0.08	21.83 ± 0.10	44.24 ± 0.12	62.34 ± 0.12

Funding

No supporting funds were provided by any sponsoring bodies for this research work.

Ethical approval

Not applicable.

Availability of the data and materials

The data related to this work has been mentioned in this manuscript.

CRediT authorship contribution statement

Muhammad Bin Ali: Visualization, Investigation, Formal analysis, Data curation. **Tehreema Iftikhar:** Writing – review & editing, Visualization, Validation, Supervision, Software, Resources, Project administration, Methodology, Investigation, Data curation, Conceptualization. **Hammad Majeed:** Writing – review & editing, Writing – original draft, Visualization, Validation, Supervision, Methodology, Investigation, Conceptualization.

Declaration of competing interest

The authors declare that they have no known competing financial interests or personal relationships that could have appeared to influence the work reported in this paper.

References

[1] I. Akhtar, et al., The role of natural products in COVID-19, in: The COVID-19 Pandemic, Apple Academic Press, 2022, pp. 393–445.
[2] F. Altaf, et al., Synthesis and performance study of Pd/CeO2 composite catalyst for enhanced MOR activity, J. Electron. Mater. 50 (12) (2021) 7222–7229.
[3] T. Iftikhar, et al., Vanilla, in: Essentials of Medicinal and Aromatic Crops, Springer, 2023, pp. 341–371.
[4] T. Iftikhar, et al., Thyme, in: Essentials of Medicinal and Aromatic Crops, Springer, 2023, pp. 399–429.
[5] M. Irfan, et al., A review on molecular scissoring with CRISPR/Cas9 genome editing technology, Toxicol. Res. 13 (4) (2024) tfae105.
[6] H. Majeed, T. Iftikhar, Ecofriendly reactive printing of cellulosic fabric with sustainable novel techniques, Cellulose 31 (11) (2024) 7067–7081.
[7] H. Majeed, T. Iftikhar, Q. Abbas, Climate resilience plastic degradation potential of Pseudomonas putida isolated from the soil of plastic waste dumping sites to reduce GHG emissions, Z. Phys. Chem. 238 (5) (2024) 797–807.
[8] N.M. Lowe, et al., Preventing and controlling zinc deficiency across the life course: a call to action, Adv. Nutr. 15 (3) (2024) 100181.
[9] S. Wang, et al., The structural characteristics of Crassostrea gigas peptide-zinc complexes and the bioactive mechanism of their enhanced zinc absorption, Food Biosci. 58 (2024) 103722.
[10] M. Xiang, et al., Association of dietary zinc consumption with periodontitis in diabetes mellitus patients: a cross-sectional study of national health and nutrition examination surveys database (2009–2014), Journal of Dental Sciences 19 (2) (2024) 952–960.
[11] H. Majeed, T. Iftikhar, K. Maqsood, Temporal and thermal dynamics exploration of different detergents' formulations components on fungal alkaliphilic lipases stability, Z. Phys. Chem. 238 (3) (2024) 563–570.
[12] H. Majeed, T. Iftikhar, K. Maqsood, Synthesis of protein-based catalyst for multi-industrial applications by using agriculture and industrial waste, Polym. Bull. 81 (14) (2024) 12633–12653.
[13] H.J. Adra, et al., Ligand-based magnetic extraction and safety assessment of zinc oxide nanoparticles in food products, J. Hazard Mater. 465 (2024) 133235.
[14] J. Fujihara, N. Nishimoto, Review of zinc oxide nanoparticles: toxicokinetics, tissue distribution for various exposure routes, toxicological effects, toxicity mechanism in mammals, and an approach for toxicity reduction, Biol. Trace Elem. Res. 202 (1) (2024) 9–23.
[15] H. Majeed, T. Iftikhar, U. Mukhtar, Novel approach to water-efficient bulk industrial textile printing production of cotton fabric, Int. J. Biol. Macromol. 262 (2024) 130064.
[16] H. Majeed, T. Iftikhar, A. Siddique, Agricultural waste upcycling into improved production of triacyl glycerol acyl hydrolases, Z. Phys. Chem. 238 (5) (2024) 809–827.
[17] H. Majeed, et al., Wild marigold, in: Essentials of Medicinal and Aromatic Crops, Springer, 2023, pp. 311–339.
[18] E.K. Kambale, et al., "Green" synthesized versus chemically synthesized zinc oxide nanoparticles: in vivo antihyperglycemic activity and pharmacokinetics, International journal of pharmaceutics 650 (2024) 123701.
[19] H. Chemingui, et al., A novel green preparation of zinc oxide nanoparticles with Hibiscus sabdariffa L.: photocatalytic performance, evaluation of antioxidant and antibacterial activity, Environ. Technol. 45 (5) (2024) 926–944.
[20] N. Naveed, et al., The global impact of COVID-19: a comprehensive analysis of its effects on various aspects of life, Toxicol. Res. 13 (2) (2024) tfae045.
[21] H. Qaiser, et al., COVID-19 pandemic and vaccines, in: M. Zia-Ul-Haq, et al. (Eds.), Alternative Medicine Interventions for COVID-19, Springer International Publishing, Cham, 2021, pp. 205–235.
[22] A. Shahbaz, et al., Porous materials: covalent Organic Frameworks (COFs) as game-changers in practical applications, a review, Rev. Inorg. Chem. 44 (1) (2024) 117–133.
[23] P. Navarro-Simarro, et al., Food and human health applications of edible mushroom by-products, New Biotechnology (2024).
[24] X.K. Wong, et al., Tiger Milk mushroom: a comprehensive review of nutritional composition, phytochemicals, health benefits, and scientific advancements with emphasis on Chemometrics and multi-omics, Food Chem. (2024) 140340.
[25] M.H. Alu'datt, et al., Designing novel industrial and functional foods using the bioactive compounds from Nigella sativa L.(black cumin): biochemical and biological prospects toward health implications, J. Food Sci. 89 (4) (2024) 1865–1893.
[26] B.D. Gebremedin, et al., Biochemical characterization of Ethiopian black cumin (Nigella sativa L.), International Journal of Food Science 2024 (1) (2024) 2746560.
[27] C.O. Ugwuoke, M. Ghali, A.A. El-Moneim, Green synthesis of carbon dots from Nigella sativa seeds for supercapacitor application, J. Energy Storage 95 (2024) 112634.
[28] P. Vinothini, et al., Potential inhibition of biofilm forming bacteria and fungi and DPPH free radicals using Tamarindus indica fruit extract assisted iron oxide nanoparticle, Inorg. Chem. Commun. 156 (2023) 111206.
[29] B. Malaikozhundan, et al., Enhanced bactericidal, antibiofilm and antioxidative response of Lawsonia inermis leaf extract synthesized ZnO NPs loaded with commercial antibiotic, Bioproc. Biosyst. Eng. 47 (8) (2024) 1241–1257.
[30] H. Majeed, et al., Tamarindus indica seed polysaccharide-copper nanocomposite: an innovative solution for green environment and antimicrobial studies, Heliyon 10 (10) (2024) e30927.
[31] M.D. Senthamarai, B. Malaikozhundan, Synergistic action of zinc oxide nanoparticle using the unripe fruit extract of Aegle marmelos (L.) - antibacterial, antibiofilm, radical scavenging and ecotoxicological effects, Mater. Today Commun. 30 (2022) 103228.
[32] S.A. Hosseini, et al., Nigella sativa extract phytochemicals: effective green/bio-active anti-corrosion agent for steel protection in saline media, Ind. Crop. Prod. 202 (2023) 116952.
[33] H. Majeed, T. Iftikhar, M. Zohaib, Extension of guava shelf life through the application of edible coating formulated with mango and lemon leaves extracts, Ind. Crop. Prod. 216 (2024) 118671.

[34] H. Majeed, T. Iftikhar, R. Abid, Green synthesis of zinc nanoparticles with plant material and their potential application in bulk industrial production of mosquito-repellent antibacterial paint formulations, React. Chem. Eng. 9 (3) (2024) 677–683.
[35] H. Majeed, T. Iftikhar, R. Abid, Green synthesis of insecticidal, bactericidal, UV absorbent, sustainable paint formulations using Mentha piperita (peppermint), React. Chem. Eng. (2024).
[36] I.G. Shitu, et al., Effects of irradiation time on the structural, elastic, and optical properties of hexagonal (wurtzite) zinc oxide nanoparticle synthesised via microwave-assisted hydrothermal route, Opt. Quant. Electron. 56 (2) (2024) 266.
[37] Y. Kudo, M. Yasuda, S. Matsusaka, Effect of particle size distribution on flowability of granulated lactose, Adv. Powder Technol. 31 (1) (2020) 121–127.
[38] A.H. Shah, M.A. Rather, Effect of calcination temperature on the crystallite size, particle size and zeta potential of TiO2 nanoparticles synthesized via polyol-mediated method, Mater. Today: Proc. 44 (2021) 482–488.
[39] M.A. Stahl, et al., Characterization and stability of α-tocopherol loaded solid lipid nanoparticles formulated with different fully hydrogenated vegetable oils, Food Chem. 439 (2024) 138149.
[40] G. Wu, et al., Potential application of novel Janus amphiphilic nanoparticles to improve the viscoelasticity of polymer solution for enhanced oil recovery, J. Dispersion Sci. Technol. (2024) 1–10.
[41] M. Hadian, et al., Characterization of chitosan/Persian gum nanoparticles for encapsulation of Nigella sativa extract as an antiviral agent against avian coronavirus, Int. J. Biol. Macromol. 265 (2024) 130749.
[42] K. Madaan, S. Sharma, A. Kalia, Effect of selenium and zinc biofortification on the biochemical parameters of Pleurotus spp. under submerged and solid-state fermentation, J. Trace Elem. Med. Biol. 82 (2024) 127365.
[43] E. Demircan, et al., 3D printable vegan plant-based meat analogue: fortification with three different mushrooms, investigation of printability, and characterization, Food Res. Int. 173 (2023) 113259.
[44] Y. Besufekad, et al., Selection of appropriate substrate for production of oyster mushroom (Pleurotus ostreatus), J. Yeast Fungal Res. 11 (1) (2020) 15–25.
[45] K.S. Luvitaa, et al., Zinc bioaccessibility in finger millet porridge blended with zinc-dense mushroom, Heliyon (2023) e18901.
[46] N.K. Kortei, et al., Infuence of gamma radiation on some textural properties of fresh and dried oyster mushrooms (Pleurotus ostreatus) (2015).
[47] H. Majeed, et al., Green synthesis of Eucalyptus globulus zinc nanoparticles and its use in antimicrobial insect repellent paint formulation in bulk industrial production, Heliyon 10 (2) (2024) e24467.
[48] R. Islam, et al., Unveiling the synthesis, characteristics, electrical conductivity, photocatalytic activity, and electrochemical activity of eco-friendly zinc oxide nanoparticles, Advanced Sensor and Energy Materials 3 (3) (2024) 100105.